This is the author's version (accepted manuscript) of a paper that has been published in Ultrasonics, Elsevier.
The final version of record is available at https://doi.org/10.1016/j.ultras.2016.11.022
G. Matrone, A. S. Savoia, G. Caliano, G. Magenes, "Depth-of-Field Enhancement in Filtered-Delay Multiply And Sum Beamformed Images Using Synthetic Aperture Focusing", Ultrasonics, vol. 75, pp. 216-225, March 2017.
DOI: 10.1016/j.ultras.2016.11.022

Depth-of-Field Enhancement in Filtered-Delay Multiply And Sum Beamformed Images Using Synthetic Aperture Focusing

Giulia Matrone[a*], Alessandro Stuart Savoia[b], Giosuè Caliano[b], Giovanni Magenes[a]

[a]*Dipartimento di Ingegneria Industriale e dell'Informazione, Università degli Studi di Pavia, Pavia, Italy*
[b]*Dipartimento di Ingegneria, Università degli Studi Roma Tre, Rome, Italy*

[*]Corresponding author (e-mail: giulia.matrone@unipv.it)

Abstract

The Synthetic Aperture Focusing (SAF) technique makes it possible to achieve a higher and more uniform quality of ultrasound images throughout depth, as if both transmit and receive dynamic focusing were applied.

In this work we combine a particular implementation of SAF, called Synthetic Transmit Aperture (STA) technique, in which a single element in turn transmits and all the array elements receive the ultrasound wave, with the Filtered-Delay Multiply and Sum (F-DMAS) non-linear beamforming algorithm that we presented in a previous paper. We show that using F-DMAS, which is based on a measure of backscattered signal spatial correlation, B-mode images have a higher contrast resolution but suffer from a loss of brightness away from the transmit focus, when a classical scan with receive-only dynamic focusing is performed. On the other hand, when synthetic transmit focusing is achieved by implementing STA, such a loss is compensated for and a higher depth of field is obtained, as signal coherence improves. A drawback of SAF/STA however is the reduced signal-to-noise ratio, due to single-element transmission; in the paper we also analyze how this influences F-DMAS images. Finally, a preliminary investigation on the use of the classical monostatic SAF technique with F-DMAS beamforming is also carried out to evaluate its potential performances.

Keywords: beamforming; Filtered-Delay Multiply And Sum; Synthetic Aperture Focusing; ultrasound medical imaging

1. INTRODUCTION

In signal processing, beamforming can be considered as a form of spatial filtering [1] aimed at reinforcing the estimate of the signal received from the direction of interest, while rejecting as much as possible interferences coming from off-axis directions.

To accomplish this task, in ultrasound medical imaging systems, the receive beamformer unit is in charge of computing and applying a set of delays and weights to the echo signals received by the transducer elements in the probe, in order to focus and steer the beam towards the desired direction, while optimizing its shape.

The standard beamforming technique implemented by commercial ultrasound scanners is the simple Delay And Sum (DAS). However, the quality of ultrasound images remains still limited by the aperture size and operating frequency of the system, which are directly related to the achievable lateral/axial resolution, depth of field (DOF) and penetration depth. On the other hand, adaptive beamformers, such as the Capon/Minimum Variance (MV) beamformer [2,3], have been developed to obtain higher resolution and contrast by controlling the aperture apodization weights based on the spatial statistics of the received signals. Other ultrasound image formation techniques have also been recently developed to improve the lateral resolution and gain a higher contrast, as, for example, the Dual Apodization with Cross-Correlation (DAX) [4] or the Side Lobe Masking [5] techniques. Besides, non-linear beamformers were proposed in the past, mainly for direction of arrival estimation but also for beam formation [6,7].

In a previous work [8], we proposed and adapted a non-linear beamforming algorithm, called Delay Multiply and Sum (DMAS), for application to ultrasound B-mode image formation. That beamformer had been originally presented by Lim *et al.* in a paper on microwave image reconstruction for breast cancer detection [9]. By introducing several further processing steps in the beamformation chain, both working on the amplitude and frequency content of the echo signals, this improved DMAS algorithm, called Filtered-DMAS (F-DMAS), was shown to achieve higher contrast resolution than DAS, both in simulation and *in vivo* tests, and also when used jointly to other ultrasound imaging techniques [10-12]. The improved performance of the F-DMAS beamformer arises from the computation of the aperture spatial auto-correlation, on which this technique is based.

This is the author's version (accepted manuscript) of a paper that has been published in Ultrasonics, Elsevier.
The final version of record is available at https://doi.org/10.1016/j.ultras.2016.11.022
G. Matrone, A. S. Savoia, G. Caliano, G. Magenes, "Depth-of-Field Enhancement in Filtered-Delay Multiply And Sum Beamformed Images Using Synthetic Aperture Focusing", Ultrasonics, vol. 75, pp. 216-225, March 2017.
DOI: 10.1016/j.ultras.2016.11.022

Actually, a slight decrease of brightness can be observed in F-DMAS B-mode images at low (i.e. near to the probe surface) and high depths, as compared to DAS. A possible explanation of this phenomenon could be that the spatial correlation of backscattered signals is higher in correspondence of the transmit focal depth. In conventional B-mode imaging, in fact, a fixed focal depth is used during transmission and dynamic focusing (DF) is usually implemented only in reception, otherwise the frame rate would be drastically reduced. An acceptable trade-off between the required frame rate and an improved image quality could be achieved by acquiring images with different transmit focal depths and splicing them together [13]; anyway, even in this case the frame rate would be reduced.

In [14] we presented some preliminary results to validate the hypothesis that the intensity loss shown by F-DMAS images away from the transmit focus could be due to the decrease of echo signal coherence when DF is applied only in reception. As a matter of fact, backscattered signal coherence is expected to reach its maximum at the transmit focus based on the Van Cittert-Zernike (VCZ) theorem [15].

A similar problem affects also Short-Lag Spatial Coherence (SLSC) imaging [16], which is another recently proposed technique based on the spatial correlation of backscattered signals [17]. SLSC computation involves the coupling, multiplying and summing of the short-lag echo signals. However, differently from B-mode image formation techniques like DMAS, in this case such operations are used to generate images of the backscattered signal spatial coherence, and not images of echo magnitudes, whose influence is removed by normalizing the cross-correlation [17]. Therefore, being SLSC images a direct representation of backscattered signals coherence, in [16] they were shown to suffer from a reduced DOF away from the transmit focal depth, based on the VCZ theorem. The DOF was instead significantly improved by implementing Synthetic Aperture Focusing (SAF) [18].

In a classical SAF implementation, the aperture is synthetically built by activating one single element at each time to act as a transmitter and receiver. Instead, when a single element is used in turn to transmit the ultrasound pulse but reception is performed by all the array elements, this technique is referred to as Synthetic Transmit Aperture (STA) [19,20]. After the transmit-receive sequence has been repeated for all the elements in the array, beamforming can be performed by synthetically focusing the acquired signals a posteriori in each point of the image space, as if implementing both transmit and receive DF. Therefore, signals can be almost

This is the author's version (accepted manuscript) of a paper that has been published in Ultrasonics, Elsevier.
The final version of record is available at https://doi.org/10.1016/j.ultras.2016.11.022
G. Matrone, A. S. Savoia, G. Caliano, G. Magenes, "Depth-of-Field Enhancement in Filtered-Delay Multiply And Sum Beamformed Images Using Synthetic Aperture Focusing", Ultrasonics, vol. 75, pp. 216-225, March 2017.
DOI: 10.1016/j.ultras.2016.11.022

correctly realigned by compensating for the two-way propagation delays at all depths, yielding to an image with higher lateral resolution, improved DOF and more uniform quality, thanks to synthetic transmit focusing. However, a drawback of these techniques is that they generally suffer from a poor SNR and low penetration capability due to single-element transmission, and also from tissue motion artifacts, due to the higher number of transmit events required to generate an image [18].

In this paper we hypothesize that there are mainly two factors that cause the decorrelation effect which affects F-DMAS image intensity in standard B-mode scans with receive-only DF, i.e.: i) the broadening of the transmit beam away from the transmit focus, and ii) noise (including both electronic noise and other interferences related to the physics of the ultrasound beam). Thus, we aim to understand how F-DMAS images are influenced by different focusing strategies. This would also provide further insights on the impact of backscattered signal coherence on F-DMAS beamforming, widening the study presented in our previous work [8]. We thus implemented F-DMAS with or without STA and synthetic transmit focusing, in order to analyze decorrelation effects in F-DMAS beamformed images.

Finally, we also investigate if F-DMAS beamforming can be used in a simpler monostatic SAF-based system, making it possible to achieve adequate imaging performance. This technique, in fact, is generally worse than STA in terms of contrast resolution, but could be more appealing for a possible hardware implementation, as it involves only one single transducer element (and thus a simpler electronics with one single channel) both to transmit and receive the ultrasound wave.

In the following pages, the F-DMAS algorithm as well as the SAF and STA techniques are first described (Section 2). Henceforth, we will use the acronym SAF to refer to the classical monostatic implementation of this technique. We then compare F-DMAS and DAS performance by reconstructing images, either with fixed transmit focus and receive-only DF, so as to emulate a classical B-mode scan, or with STA and synthetic transmit focusing (i.e. emulating both transmit and receive dynamic focusing), and we evaluate the results achieved in simulations, phantom experiments and *in vivo* (Section 3). The performance of classical SAF together with F-DMAS is analyzed in phantom experiments too. Finally, in Section 4 we discuss the results and provide some conclusive remarks.

This is the author's version (accepted manuscript) of a paper that has been published in Ultrasonics, Elsevier.
The final version of record is available at https://doi.org/10.1016/j.ultras.2016.11.022
G. Matrone, A. S. Savoia, G. Caliano, G. Magenes, "Depth-of-Field Enhancement in Filtered-Delay Multiply And Sum Beamformed Images Using Synthetic Aperture Focusing", Ultrasonics, vol. 75, pp. 216-225, March 2017.
DOI: 10.1016/j.ultras.2016.11.022

2. MATERIALS AND METHODS

2.1. SAF and STA techniques

The classical monostatic implementation of SAF consists in activating each time a single element of the array to transmit an unfocused spherical wave and to receive the echo signal. If we consider N transducers and we denote the active element with index i (i=1…N), then a set of raw radiofrequency (RF) signals $\boldsymbol{V}$ is collected after all elements have been used one by one to transmit and receive:

$$\boldsymbol{V}(t) = \left[v_1(t) \quad v_2(t) \quad \ldots \quad v_N(t) \right]. \tag{1}$$

Each column v_i of matrix $\boldsymbol{V}$ represents the RF signal received by element i after it has transmitted.

In order to realign the received signals v_i, the focusing delays τ_{ii} are computed by considering the two-way distance from element i to the focal point and vice-versa. For example, focusing delay τ_{ii} is computed as follows (Fig. 1a):

$$\tau_{ii} = \tau_{i,TX} + \tau_{i,RX} = \frac{2}{c}\sqrt{(x_F - x_i)^2 + z_F^2}\,, \tag{2}$$

where $\tau_{i,TX}$ and $\tau_{i,TX}$ are the transmit and receive delay of element i, respectively, the coordinates of the active element are (x_i, z_i=0), and the focus is placed at (x_F, z_F); c is the sound speed in the medium. In this way, a new set $\boldsymbol{S}$ of focused signals is obtained:

$$\boldsymbol{S}(t) = \left[s_1(t) \quad s_2(t) \quad \ldots \quad s_N(t) \right] \tag{3}$$

where $s_i(t) = v_i(t - \tau_{ii})$.

In order to implement STA, instead, we use the following procedure. Each single transducer element in the active aperture is used in turn to transmit an un-focused spherical wave, and the backscattered echo signals are received by all elements; this process is repeated for each transducer in the aperture. If index i refers to the transmitting element and j=1…N to the receiving elements, then a set of RF signals $\boldsymbol{V}_i$ is collected by the N receivers for each i-th transmission:

$$\boldsymbol{V}_i(t) = \left[v_{i1}(t) \quad v_{i2}(t) \quad \ldots \quad v_{iN}(t) \right], \tag{4}$$

This is the author's version (accepted manuscript) of a paper that has been published in Ultrasonics, Elsevier.
The final version of record is available at https://doi.org/10.1016/j.ultras.2016.11.022
G. Matrone, A. S. Savoia, G. Caliano, G. Magenes, "Depth-of-Field Enhancement in Filtered-Delay Multiply And Sum Beamformed Images Using Synthetic Aperture Focusing", Ultrasonics, vol. 75, pp. 216-225, March 2017.
DOI: 10.1016/j.ultras.2016.11.022

where each column v_{ij} of the matrix represents the RF signal received by element j when element i transmits. In order to realign these signals, delays τ_{ij} are computed by considering the two-way distance from the transmitting element i to the focal point, and back to each receiving element j (Fig. 1b), as follows:

$$\tau_{ij} = \tau_{i,TX} + \tau_{j,RX} = \frac{1}{c}\left[\sqrt{(x_F - x_i)^2 + z_F^2} + \sqrt{(x_F - x_j)^2 + z_F^2}\right], \tag{5}$$

where the coordinates of the transmitting element are (x_i, z_i=0), those of the receiving element are (x_j, z_j=0) and $\tau_{i,TX}$ and $\tau_{j,TX}$ are the transmit and receive delay of elements i and j, respectively. The new set $\boldsymbol{U}_i$ of focused signals is given by:

$$\boldsymbol{U}_i(t) = [u_{i1}(t) \quad u_{i2}(t) \quad \ldots \quad u_{iN}(t)] \tag{6}$$

where $u_{ij}(t) = v_{ij}(t - \tau_{ij})$. The transmit-receive sequence is repeated for each i-th element in the aperture and the N realigned signal sets $\boldsymbol{U}_i$ are summed together:

$$\boldsymbol{S}(t) = \sum_{i=1}^{N} \boldsymbol{U}_i(t) = [s_1(t) \quad s_2(t) \quad \ldots \quad s_N(t)], \quad \text{with} \quad s_j(t) = \sum_{i=1}^{N} u_{ij}(t) \tag{7}$$

so that one single signal $s_j(t)$ is obtained for each j-th receiving element in the aperture.

Both in the case of SAF and STA, the signals $\boldsymbol{S}$ obtained respectively in (3) and (7) are subsequently used for image formation by applying the considered beamforming algorithm: for F-DMAS, the processing steps described in the next section are applied, while for DAS the signals are simply summed up:

$$y_{DAS}(t) = \sum_{j=1}^{N} s_j(t). \tag{8}$$

Since with SAF and STA the synthetic focusing stage is totally (i.e. both for transmit and receive, eq. 3 and 6) implemented a-posteriori on the raw signal set, the advantage of these techniques is that they make it possible to vary the focal point with depth, and therefore both transmit and receive DF may be implemented. This allows us to considered also a third configuration in this work, in which STA is implemented by synthetizing a focal point (x_F, z_F^*) with fixed depth (i.e. z_F= z_F^*) and varying only the receive focus (x_F, z_F) with depth, so as to emulate a B-mode scan. In this case the delays are computed as follows (Fig. 1c):

$$\tau_{ij} = \tau_{i,TX} + \tau_{j,RX} = \frac{1}{c}\left[\sqrt{(x_F - x_i)^2 + z_F^{*2}} + \sqrt{(x_F - x_j)^2 + z_F^2}\right]. \tag{9}$$

This is the author's version (accepted manuscript) of a paper that has been published in Ultrasonics, Elsevier.
The final version of record is available at https://doi.org/10.1016/j.ultras.2016.11.022
G. Matrone, A. S. Savoia, G. Caliano, G. Magenes, "Depth-of-Field Enhancement in Filtered-Delay Multiply And Sum Beamformed Images Using Synthetic Aperture Focusing", Ultrasonics, vol. 75, pp. 216-225, March 2017.
DOI: 10.1016/j.ultras.2016.11.022

Of course SAF and STA have both pros and cons. For example, with SAF, each signal s_i is the result of one single transmit-receive event and (with DAS) the beampattern has a narrower main lobe, high side and grating lobes, as shown in [19]. With STA instead, each output signal s_j is obtained by combining the contributions of all the aperture transmitting elements (7) and the beampattern has lower side lobes, no grating lobes, but a

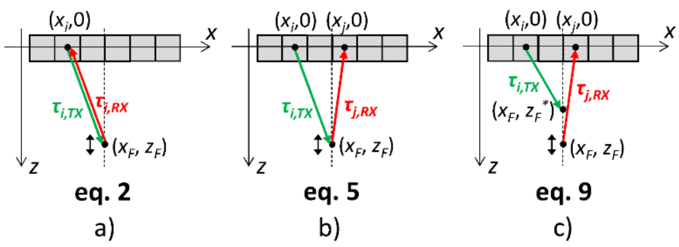

Fig. 1. Schematic representation of delay calculation, corresponding to: a) equation (2), b) equation (5), c) equation (9).

wider main lobe [19]. Anyway, SAF could be very attractive for its simpler hardware implementation, especially if used in conjunction with a beamforming algorithm as F-DMAS, which is expected to improve its performances in terms of contrast resolution.

2.2. Filtered-Delay Multiply And Sum beamforming

After the signal focusing/delaying phase, the following procedure is applied to implement F-DMAS [8]. First, the signed squared root is applied to the realigned RF signals s_j, which are then combinatorially coupled, multiplied and summed. In the practice, it is as if a new set of "equivalent RF signals" is computed, whose amplitude has been rescaled just before entering the multiplication stage:

$$\hat{s}_j(t) = sign(s_j(t)) \cdot \sqrt{|s_j(t)|}. \tag{10}$$

Hence, the DMAS beamformed signal is given by:

$$y_{DMAS}(t) = \sum_{n=1}^{N-1} \sum_{m=n+1}^{N} \hat{s}_n(t)\hat{s}_m(t). \tag{11}$$

In [8] we explain that this operation is equivalent to the aperture spatial auto-correlation, except for the fact that the new set of RF signals (10) is employed in the calculation, the auto-products (n=m) are not considered and each signal couple is used only once (i.e., $s_n s_m$ and not $s_m s_n$). As the multiplication stage also changes the frequency content of the output signal y_{DMAS}, a final band-pass (BP) filtering stage is implemented to generate

This is the author's version (accepted manuscript) of a paper that has been published in Ultrasonics, Elsevier.
The final version of record is available at https://doi.org/10.1016/j.ultras.2016.11.022
G. Matrone, A. S. Savoia, G. Caliano, G. Magenes, "Depth-of-Field Enhancement in Filtered-Delay Multiply And Sum Beamformed Images Using Synthetic Aperture Focusing", Ultrasonics, vol. 75, pp. 216-225, March 2017.
DOI: 10.1016/j.ultras.2016.11.022

the beamformed output $y_{F\text{-}DMAS}$. The filter is designed to pass only the second harmonics almost unaltered while attenuating the lower and higher spectral components, especially the baseband one.

The spatial autocorrelation of a N-element aperture with uniform weights (i.e. a *rect* function) is a triangle made of $2N-1$ coefficients. This means that the contribution of short-lag coefficients, obtained by cross-correlating signals received by close elements in the array, is higher than that of long-lag ones. We shall also consider that, the higher the lag between the elements, the less the RF signals will be correlated; therefore, a higher contribution is provided by more strongly correlated signal couples. The described operations make it possible to achieve several advantages compared to DAS:

1) images have a higher lateral resolution, since it is as if a wider aperture is employed (the auto-correlation has $2N$-1 coefficients) and the central frequency is doubled;
2) side lobes are lowered thanks to the cross-correlation (i.e. couple and multiply) stage, which turns out into a higher contrast resolution;
3) for the same reason, un-correlated noise is better rejected.

In order to generate the desired B-mode image, the focusing and beamforming (i.e. F-DMAS or DAS) processing steps are repeated for each scan line, and the image lines are then demodulated by applying the Hilbert transform. Each image is normalized to its maximum value, logarithmically compressed, interpolated and finally displayed.

2.3. Influence of focusing strategies on the coherence of received signals

To understand the expected decrease of echo signal correlation in B-mode images away from the transmit focus when DF is applied only in reception, and consequently the loss of amplitude in the F-DMAS image, the VCZ theorem should be recalled.

The VCZ theorem provides a theoretical basis for the calculation of the spatial coherence of backscattered signals. In [15,21] it was applied to ultrasound, and it was demonstrated that the spatial correlation function of the pressure field produced by an incoherent source (such as diffuse scatterers) is proportional to the Fourier transform of the source intensity distribution. For discrete time signals, assuming that the source is incoherent

This is the author's version (accepted manuscript) of a paper that has been published in Ultrasonics, Elsevier.
The final version of record is available at https://doi.org/10.1016/j.ultras.2016.11.022
G. Matrone, A. S. Savoia, G. Caliano, G. Magenes, "Depth-of-Field Enhancement in Filtered-Delay Multiply And Sum Beamformed Images Using Synthetic Aperture Focusing", Ultrasonics, vol. 75, pp. 216-225, March 2017.
DOI: 10.1016/j.ultras.2016.11.022

and quasi-monochromatic, and that no phase aberrations are present, the sample spatial correlation R of the ultrasound field evaluated at two points (e.g., at two array elements E_1 and E_2) can be approximated as [21,22]:

$$R \approx e^{-j2\pi f_0 \tau} \sum_{m=1}^{M} I_m e^{-j2\pi x_m \frac{(x_1 - x_2)}{\lambda_0 z}} , \tag{12}$$

where M discrete point sources are considered; x_m, x_1 and x_2 are the lateral spatial coordinates respectively of the m-th source, of element E_1 or element E_2, f_0 is the center frequency, $\lambda_0 = c/f_0$, I_m is the ultrasound field intensity at the m-th point, and z is the distance between the source and the aperture (z is assumed to be much greater than the aperture dimension).

In (12), the summation term is the discrete Fourier transform of the source intensity distribution. The phase term outside the summation instead corresponds to the time delay to be applied for focusing at point m; consequently, this term cancels if signals are properly phased shifted (i.e. realigned) for focusing during reception. When τ=0, the aperture autocorrelation function is the Fourier transform of the field intensity; therefore, for a uniformly weighted/apodized aperture, the field in the focal plane is a $sinc^2$ and the spatial correlation is a triangle function. This means that, the wider the beam is (e.g. away from the focus), the narrower the autocorrelation function becomes [22].

For this reason, spatial coherence is maximized only at the focus, where the beam is narrower than at other depths. This is the case of conventional B-mode imaging, where the receive beamformer correctly compensates for the two-way propagation delays only at the transmit focus, as DF is applied only in reception. On the other hand, SAF/STA makes it possible to implement synthetic transmit focusing, and the backscattered signals can be correctly realigned at each time instant; thus, the aperture autocorrelation is expected to improve at all depths [16].

2.4. Simulation and experimental setup

The results obtained by applying DAS and F-DMAS beamforming to reconstruct images, either with receive-only DF or with STA and synthetic transmit focusing, were compared in simulated and experimental conditions. Finally, an analysis on the performance of SAF with F-DMAS was carried out in experimental phantom scans.

This is the author's version (accepted manuscript) of a paper that has been published in Ultrasonics, Elsevier.
The final version of record is available at https://doi.org/10.1016/j.ultras.2016.11.022
G. Matrone, A. S. Savoia, G. Caliano, G. Magenes, "Depth-of-Field Enhancement in Filtered-Delay Multiply And Sum Beamformed Images Using Synthetic Aperture Focusing", Ultrasonics, vol. 75, pp. 216-225, March 2017.
DOI: 10.1016/j.ultras.2016.11.022

A 192-element linear array (element width=215 µm, height=5 mm, kerf=30 µm), with a center operating frequency of 5 MHz, was modelled in Matlab for simulations using Field II [23,24]. The elevation focus was fixed at 23.5 mm. A 64-element active aperture was considered and 129 lines were scanned (scan line spacing = 1 pitch). In the case of receive-only DF, the fixed focus in transmission was set at z=24 mm. The F-number (F#) in all cases varied with depth, as no dynamic apodization was applied in reception and the full aperture was always used.

Received signals were first BP pre-filtered by simply windowing their spectrum; when F-DMAS was used, a further BP filter was applied to the beamformed lines. The parameters of the filters were empirically determined by observing the signal spectra and they are given in Table 1. In the simulations, a 2-cycle, Gaussian-windowed sinusoidal burst at 5 MHz (fractional bandwidth ≈ 70%) was employed as excitation signal, with a sampling frequency of 50 MHz.

First, a numerical phantom scan was simulated. The phantom was homogeneous; it was made of 150,000 scattering points with a Gaussian-distributed reflectivity, randomly spread in a 12x1x40 mm^3 volume, centered at (x, y, z)=(0, 0, 30) mm.

Experimental acquisitions were performed by connecting a linear array probe (model LA-532, Esaote s.p.a.,Florence, Italy) to the ULA-OP system [25] and using the same scan parameters set in simulations.

TABLE 1. Parameters of the BP-filters.

	Filter	**Window**	**Frequency boundaries**
Simulations	RF signals pre-filter	Tukey (α=0.5)	1.5–9 MHz
	F-DMAS final filter	Tukey (α=0.5)	3–15 MHz
Experiments	RF signals pre-filter	Tukey (α=0.3)	1.4–7 MHz
	F-DMAS final filter	Tukey (α=0.5)	3.3–13 MHz

Actually, a custom routine was developed to implement the SAF/STA transmit-receive sequence with ULA-OP, by activating each time only one element to transmit and receiving with all the array. The voltage

This is the author's version (accepted manuscript) of a paper that has been published in Ultrasonics, Elsevier.
The final version of record is available at https://doi.org/10.1016/j.ultras.2016.11.022
G. Matrone, A. S. Savoia, G. Caliano, G. Magenes, "Depth-of-Field Enhancement in Filtered-Delay Multiply And Sum Beamformed Images Using Synthetic Aperture Focusing", Ultrasonics, vol. 75, pp. 216-225, March 2017.
DOI: 10.1016/j.ultras.2016.11.022

excitation signal was a 5 MHz, 2-cycle, Hanning-windowed sinusoidal burst, with a 64 V_{pp} amplitude. The sampling frequency was 50 MHz.

A CIRS phantom model 040GSE (CIRS Inc., Norfolk, VA) was scanned to obtain an image of anechoic cysts at different depths and also of a homogeneous region, for comparison with simulations; raw pre-beamforming data were then processed in Matlab for offline image reconstruction. In the case of the homogeneous-region scan, a further set of images was generated by artificially worsening the quality of RF signals used for reconstruction, so as to investigate the performance of F-DMAS in noisier conditions. To do so, synthetic white noise (Gaussian distribution, SNR=40 dB) was added to the raw RF signals in Matlab. A time/depth-varying gain of 2.5 dB/cm was applied to the noise signal, since this was the same gain set for Time Gain Compensation (TGC) in the ULA-OP system during acquisitions.

Finally, *in vivo* images of the human carotid artery were acquired; here the transmit focal depth (for the receive-only DF case) was set to z=15 mm.

By synthetizing the focusing delays as in eq. 9 or eq. 2/5, it was thus possible to use the same set of RF-signals (and thus to perform a single acquisition) to reconstruct images both with receive-only DF or with SAF/STA with synthetic transmit focusing (i.e. transmit/receive dynamic focusing), respectively.

For cyst phantom images, three parameters were measured for performance evaluation, i.e. the contrast ratio (CR), contrast-to-noise ratio (CNR) and SNR parameters; they were computed as follows [17]:

$$CR = 20\,log_{10}\left(\frac{\mu_{cyst}}{\mu_{bck}}\right) \tag{13}$$

$$CNR = \frac{\left|\mu_{bck} - \mu_{cyst}\right|}{\sqrt{\sigma_{bck}^2 + \sigma_{cyst}^2}} \tag{14}$$

$$SNR = \frac{\mu_{bck}}{\sigma_{bck}} \tag{15}$$

where μ_{cyst} and μ_{bck} are the mean image values measured on the envelope-detected signals (before log-compression) respectively inside the cyst and in the surrounding background, and σ_{cyst}, σ_{bck} are the corresponding standard deviations.

This is the author's version (accepted manuscript) of a paper that has been published in Ultrasonics, Elsevier.
The final version of record is available at https://doi.org/10.1016/j.ultras.2016.11.022
G. Matrone, A. S. Savoia, G. Caliano, G. Magenes, "Depth-of-Field Enhancement in Filtered-Delay Multiply And Sum Beamformed Images Using Synthetic Aperture Focusing", Ultrasonics, vol. 75, pp. 216-225, March 2017.
DOI: 10.1016/j.ultras.2016.11.022

3. RESULTS

3.1. Simulated homogeneous phantom images

Fig. 2 represents the images of the phantom obtained with DAS and F-DMAS by implementing receive-only DF or STA with synthetic transmit focusing.

As expected, in the first case (Fig. 2a-b) the image intensity lowers away from the transmit focal depth (i.e. z=24 mm). This intensity loss is visibly more pronounced in the F-DMAS image (Fig. 2b). On the other hand, with synthetic transmit focusing, not only the peak intensities of both the DAS and F-DMAS images are more uniform at all depths (Fig. 2c-d), but they are also very similar all along the z axis. A higher contrast resolution can be always observed in the case of F-DMAS (Fig. 2b, d) as the speckle pattern looks better defined.

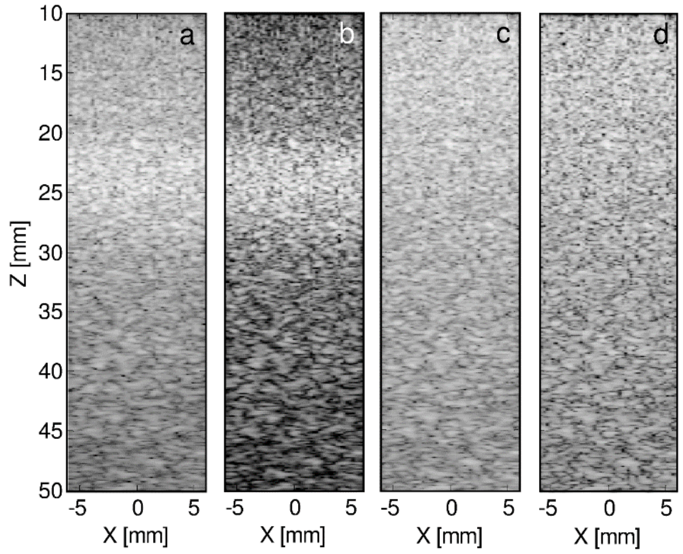

Fig. 2. Simulated images of the numerical homogeneous phantom, acquired by implementing receive-only DF (a, b) or STA with synthetic transmit focusing (c, d), and DAS (a, c) or F-DMAS (b, d) beamforming. Images are displayed over a 60 dB dynamic range.

3.2. Experimental homogeneous phantom images

The same test was carried out also on experimental data, by acquiring images of a homogeneous area of the CIRS phantom. The phantom images in the four considered conditions (i.e. receive-only DF or STA with synthetic transmit focusing, and with DAS or F-DMAS) are represented in Fig. 3.

This is the author's version (accepted manuscript) of a paper that has been published in Ultrasonics, Elsevier.
The final version of record is available at https://doi.org/10.1016/j.ultras.2016.11.022
G. Matrone, A. S. Savoia, G. Caliano, G. Magenes, "Depth-of-Field Enhancement in Filtered-Delay Multiply And Sum Beamformed Images Using Synthetic Aperture Focusing", Ultrasonics, vol. 75, pp. 216-225, March 2017.
DOI: 10.1016/j.ultras.2016.11.022

In both the focusing modalities, F-DMAS performs better than DAS in terms of image contrast resolution (Fig. 3b, d). Moreover, in the synthetic transmit focusing case (Fig. 3c, d) the speckle peak intensities of the two images become similar at all depths.

When F-DMAS is used in conjunction with STA and synthetic transmit focusing in the noisier case, the amplitude loss shown by the image with receive-only DF away from the transmit focal depth is compensated for, but only partially. Actually, at higher depths the results are quite different from the original images, and a lower intensity is still shown by synthetic-transmit-focusing images with F-DMAS.

The image maximum amplitudes at each depth may be thus analyzed to effectively highlight the different behavior of F-DMAS in the two focusing modalities, and also in the original and noisier conditions. The speckle peak values (in the x = [-1; 1] mm range) were detected in each DAS/F-DMAS image of the homogeneous phantom, and plotted in Fig. 4. Overall, Fig. 4 confirms that with receive-only DF the difference between DAS and F-DMAS maximum image amplitudes is low only near to the focal depth, while before and after the transmit focus it reaches values higher than 10-15 dB (Fig. 4a, c). On the other hand, the plots in Fig. 4b show that this difference is very low at all depths for original images with synthetic transmit focusing in Fig. 3c-d. This is not true in the case of images with synthetic transmit focusing and additive noise. In Fig. 4d

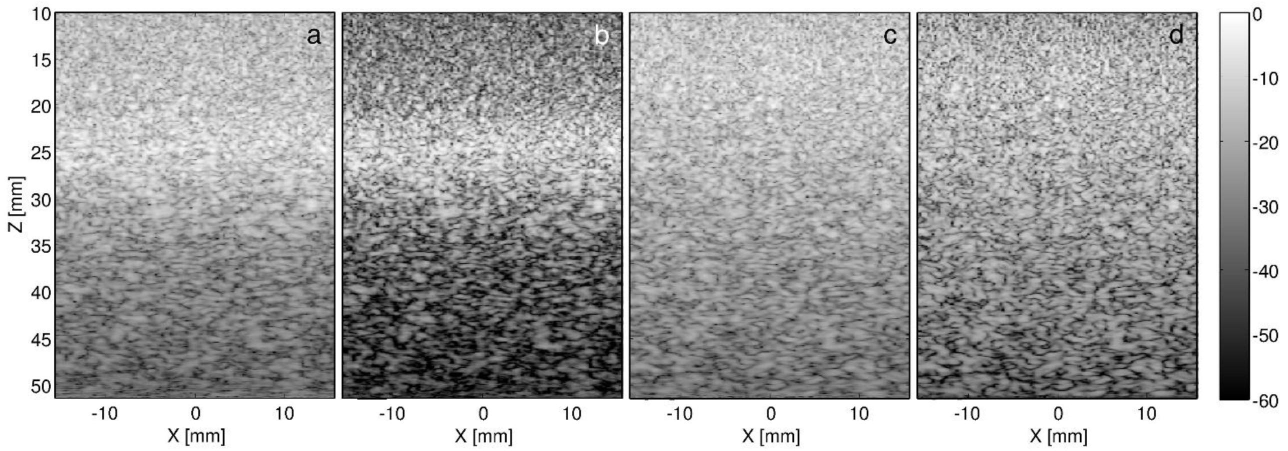

Fig. 3. Homogeneous phantom images, experimentally acquired by implementing receive-only DF (a, b) or STA with synthetic transmit focusing (c, d), with DAS (a, c) or F-DMAS (b, d) beamforming. Images are displayed over a 60 dB dynamic range.

This is the author’s version (accepted manuscript) of a paper that has been published in Ultrasonics, Elsevier.
The final version of record is available at https://doi.org/10.1016/j.ultras.2016.11.022
G. Matrone, A. S. Savoia, G. Caliano, G. Magenes, “Depth-of-Field Enhancement in Filtered-Delay Multiply And Sum Beamformed Images Using Synthetic Aperture Focusing”, Ultrasonics, vol. 75, pp. 216-225, March 2017.
DOI: 10.1016/j.ultras.2016.11.022

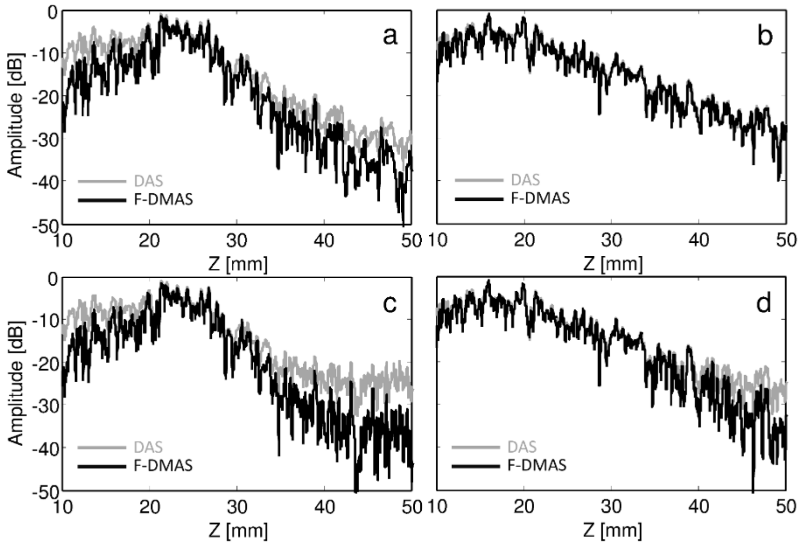

Fig. 4. Maximum amplitudes of the DAS and F-DMAS images of the CIRS uniform phantom in the *x*=[-1; 1] mm range, with receive-only DF (a, c) or STA and synthetic transmit focusing (b, d), and with DAS (gray lines) or F-DMAS (black line). Panels (c, d) refer to images generated from RF signals with synthetic additive white noise.

in fact the difference between DAS and F-DMAS also increases at depths close to 40-50 mm, reaching again values higher than 10 dB, due to the lower amplitude of the F-DMAS image, caused by noise. Also close to the probe (i.e. z<15 mm), the difference between the DAS and F-DMAS images slightly increases in Fig. 4b,d, due to the fixed receive apodization scheme, which implies the use of a low-F# focused aperture, causing an increased decorrelation.

3.3. Experimental cyst phantom images

Acquisitions of phantom images with cysts at increasing depths were also performed in order to analyze the CR, CNR and SNR. The experimental phantom images are shown in Fig. 5; the circular regions (3 mm diameter) marked on Fig. 5a enclose the image areas used to compute the CR, CNR and SNR. In this experiment, the RF signals relative to 12 consecutive frames were averaged, before doing image reconstruction, to improve the SNR at higher depths. This number was empirically chosen in order to improve the quality of images at higher depths as much as needed, by suppressing electronic noise. Albeit such procedure would be unfeasible in a real-time application, due to the too high signal acquisition time and memory resources required, frame averaging allows us to analyze the DOF improvement with STA in more

This is the author’s version (accepted manuscript) of a paper that has been published in Ultrasonics, Elsevier.
The final version of record is available at https://doi.org/10.1016/j.ultras.2016.11.022
G. Matrone, A. S. Savoia, G. Caliano, G. Magenes, “Depth-of-Field Enhancement in Filtered-Delay Multiply And Sum Beamformed Images Using Synthetic Aperture Focusing”, Ultrasonics, vol. 75, pp. 216-225, March 2017.
DOI: 10.1016/j.ultras.2016.11.022

ideal conditions, i.e. in the presence of acoustical noise only (e.g. clutter, aberrations, etc.) and with an as low as possible electronic noise.

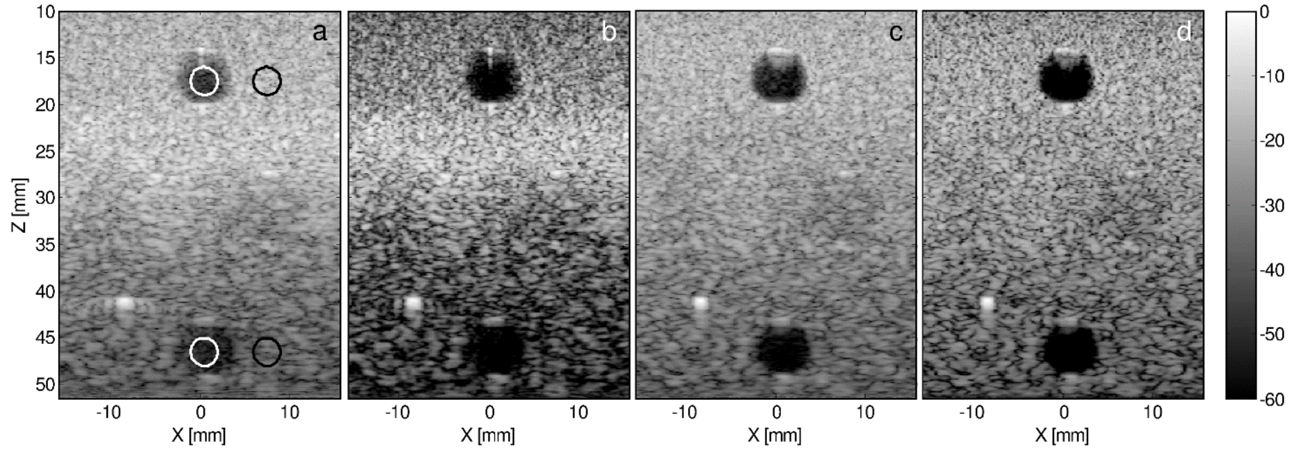

Fig. 5. Cyst phantom images, experimentally acquired by implementing receive-only DF (a, b) or STA with synthetic transmit focusing (c, d), with DAS (a, c) or F-DMAS (b, d) beamforming and frame averaging. Images are displayed over a 60 dB dynamic range.

Again, the STA images with F-DMAS and synthetic transmit focusing (Fig. 5d) show a compensation of the speckle amplitude at lower and higher depths, with respect to the receive-only DF case (Fig. 5b). The contrast resolution of the F-DMAS images is always higher than with DAS; besides, with synthetic transmit focusing this higher quality is achieved more uniformly at all depths.

As reported in Table 2, the CR with F-DMAS is in any case higher (in absolute value) than with DAS. When STA with synthetic transmit focusing is implemented, the CR increases with respect to the receive-only DF case, especially for the F-DMAS image. Furthermore, the difference between the CR values measured at z=17.5 mm and z=46.5 mm in the F-DMAS image decreases from 17.6 dB with receive-only DF to 7.4 dB with synthetic transmit focusing, becoming similar to the value obtained with DAS (i.e. 7.7 dB).

This is the author's version (accepted manuscript) of a paper that has been published in Ultrasonics, Elsevier.
The final version of record is available at https://doi.org/10.1016/j.ultras.2016.11.022
G. Matrone, A. S. Savoia, G. Caliano, G. Magenes, "Depth-of-Field Enhancement in Filtered-Delay Multiply And Sum Beamformed Images Using Synthetic Aperture Focusing", Ultrasonics, vol. 75, pp. 216-225, March 2017.
DOI: 10.1016/j.ultras.2016.11.022

TABLE 2. CR, CNR and SNR values for the experimental cyst phantom images shown in Fig. 5 and 7

Beamformer	**z [mm]**	**Receive-only DF (frame averaging) (Fig. 5)**			**STA with synthetic transmit focusing (frame averaging) (Fig. 5)**			**SAF with synthetic transmit focusing (frame averaging) (Fig. 7)**			**SAF with synthetic transmit focusing (single frame) (Fig. 7)**		
		CR [dB]	**CNR**	**SNR**	**CR [dB]**	**CNR**	**SNR**	**CR [dB]**	**CNR**	**SNR**	**CR [dB]**	**CNR**	**SNR**
DAS	17.5	-28.9	1.84	1.91	-34	1.81	1.85	-7.9	1.03	1.85	-8	1.03	1.83
F-DMAS	17.5	-41.2	1.06	1.07	-47.1	1.39	1.39	-13.6	0.75	0.97	-13.6	0.75	0.96
DAS	46.5	-14.2	1.72	2.17	-26.3	2.04	2.15	-8.6	1.14	1.98	-4.8	0.71	1.87
F-DMAS	46.5	-23.6	1.14	1.22	-39.7	1.84	1.86	-14.6	0.85	1.06	-9.4	0.63	0.98

The CNR and SNR values for F-DMAS are instead always lower than for DAS. Since F-DMAS is designed to suppress incoherent contributions in the backscattered signals received by the aperture, the beam has lower side-lobes and a narrower main-lobe, which makes the Point Spread Function (PSF) sharper and the contrast resolution improve. This is why the speckle pattern looks "finer" and many more dark regions appear in the image instead of grey areas (compared to DAS), which turns out into a decrease of the CNR [3,8,26].

3.4. Evaluation of monostatic SAF performance with F-DMAS

In order to analyze also the performance of F-DMAS combined with the simpler monostatic SAF technique, the simulated beampatterns obtained with STA and SAF (applying synthetic transmit focusing in both cases) were compared. Fig. 6 shows that, as expected, the SAF beampattern has a narrower main lobe but higher side lobes compared to STA. However, thanks to F-DMAS, the contrast-resolution performance of SAF can be significantly improved, achieving a beampattern with a side-lobe level under -60 dB and an even narrower main lobe.

For what concerns phantom scans, Fig. 7 shows both the single-frame images and those reconstructed by averaging the RF signals of 12 frames (for comparison with Fig. 5). In fact, in the case of classical monostatic SAF, which is much more critical from a SNR point of view compared to STA, it could be interesting to take into account the effect of electronic noise. Besides, as we are investigating SAF for its simpler hardware implementation, the single-frame images should be considered, as these are the ones that would be obtained in a real application.

This is the author's version (accepted manuscript) of a paper that has been published in Ultrasonics, Elsevier.
The final version of record is available at https://doi.org/10.1016/j.ultras.2016.11.022
G. Matrone, A. S. Savoia, G. Caliano, G. Magenes, "Depth-of-Field Enhancement in Filtered-Delay Multiply And Sum Beamformed Images Using Synthetic Aperture Focusing", Ultrasonics, vol. 75, pp. 216-225, March 2017.
DOI: 10.1016/j.ultras.2016.11.022

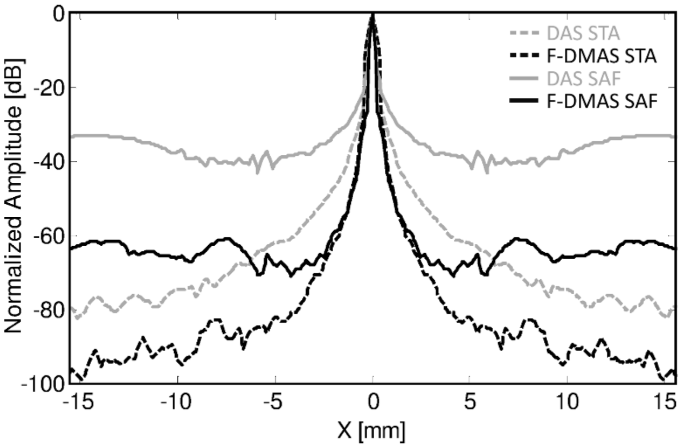

Fig. 6. Simulated beampatterns at 24 mm depth, obtained by implementing STA (dashed lines) or SAF (solid lines) with DAS (gray lines) or F-DMAS (black lines) beamforming.

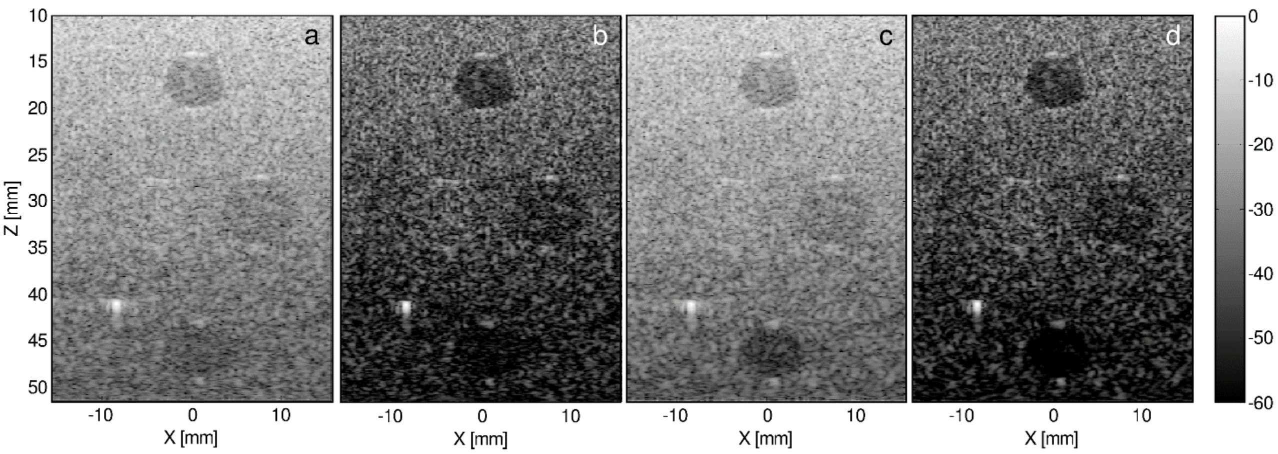

Fig. 7. Cyst phantom images, experimentally acquired by implementing a SAF scan with synthetic transmit focusing, DAS (a, c) or F-DMAS (b, d) beamforming, and without (a, b) or with (c, d) frame averaging. Images are displayed over a 60 dB dynamic range.

When SAF is applied together with F-DMAS, the quality of the cyst phantom image in Fig. 7 improves in terms of CR (Table 2). The cysts look darker with F-DMAS and the boundaries of the more superficial cyst are better defined. The speckle pattern is finer compared to the STA case; this effect is to be expected, as the SAF beampattern has a narrower main lobe, especially when F-DMAS is employed.

Overall, the F-DMAS images look much darker, since the side-lobe contribution, whose presence is significant in the DAS images, is lowered. For a similar reason, the black cyst at higher depths is hardly

This is the author's version (accepted manuscript) of a paper that has been published in Ultrasonics, Elsevier.
The final version of record is available at https://doi.org/10.1016/j.ultras.2016.11.022
G. Matrone, A. S. Savoia, G. Caliano, G. Magenes, "Depth-of-Field Enhancement in Filtered-Delay Multiply And Sum Beamformed Images Using Synthetic Aperture Focusing", Ultrasonics, vol. 75, pp. 216-225, March 2017.
DOI: 10.1016/j.ultras.2016.11.022

detectable in the F-DMAS images; in this region, in fact, the received signal SNR is low, and therefore many dark areas appear in the background speckle where the clutter is suppressed by F-DMAS.

Frame averaging improves image quality, most of all in the deeper regions (Table 2). Anyway, even in the single-frame case (Fig. 7a-b), the pixels inside the deeper cyst are darker with F-DMAS and a higher CR is achieved compared to DAS.

It is also worth pointing out that with SAF, thanks to the improved detail resolution (i.e. narrower main lobe), the borders of cysts are better highlighted, which improves the visibility of a further cyst (at 30-35 mm depth) in Fig. 7, which instead was hardly noticeable in Fig. 5.

3.5. In vivo images of the carotid artery

In order to further validate the obtained results, Fig. 8 shows the *in vivo* single-frame images of the human carotid artery, obtained by implementing receive only DF or STA with synthetic transmit focusing, and with DAS or F-DMAS.

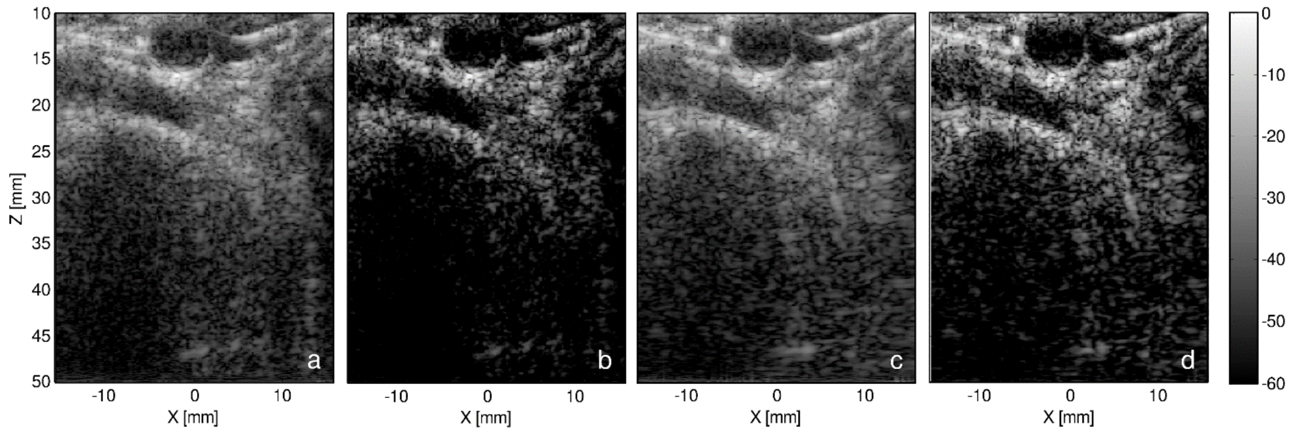

Fig. 8. *In vivo* images (single-frame) of the carotid artery, obtained by implementing receive-only DF (a, b) or STA with synthetic transmit focusing (c, d), and by applying DAS (a, c) or F-DMAS (b, d) beamforming. Images are displayed over a 60 dB dynamic range.

In Fig. 8b, it can be seen that the F-DMAS image with receive-only DF shows a reduced intensity away from the transmit focus (i.e. z=15 mm), especially in the higher depth regions. This is also confirmed by the plots represented in Fig. 9a (actually in Fig. 9 we preferred to plot the image axial sections at x=-10 mm and not the difference between the peak amplitudes, as in Fig. 4, since in this case the tissues are not homogeneous).

This is the author's version (accepted manuscript) of a paper that has been published in Ultrasonics, Elsevier.
The final version of record is available at https://doi.org/10.1016/j.ultras.2016.11.022
G. Matrone, A. S. Savoia, G. Caliano, G. Magenes, "Depth-of-Field Enhancement in Filtered-Delay Multiply And Sum Beamformed Images Using Synthetic Aperture Focusing", Ultrasonics, vol. 75, pp. 216-225, March 2017.
DOI: 10.1016/j.ultras.2016.11.022

Such an effect is however compensated for by synthetic transmit focusing (Fig. 8d and 9b), making the anatomical structures more visible at all depths. Compared to DAS, F-DMAS images show in every case a better contrast resolution and clutter suppression.

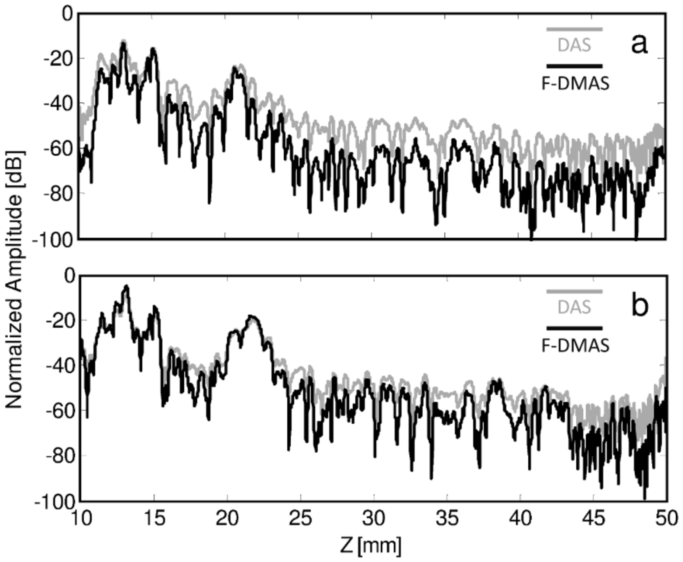

Fig. 9. Plot of the axial sections (at *x*=-10 mm) of the carotid artery images in Fig. 8: a) receive-only DF, or b) STA with synthetic transmit focusing. Gray and black lines refer respectively to DAS and F-DMAS images.

4. DISCUSSION AND CONCLUSION

The initial hypothesis made in this work was that the reduced pixel intensity shown by B-mode F-DMAS images away from the transmit focus, compared to DAS (Fig. 2a-b), could be related to a decorrelation effect, caused by the broadening of the transmit beam when DF is implemented only in reception. To confirm this assumption, a SAF technique is required, which makes it possible to beamform the received signals as if they are dynamically focused both in transmission and reception; in a classical B-mode scan, in fact, this would not be practically feasible without drastically limiting the frame rate. We thus compare the results obtained by applying F-DMAS to data acquired in different scenarios by implementing STA, both with receive-only DF and synthetic transmit focusing (which allows us to compare these two different focusing modes on the same set of RF signals, acquired by performing one single scan of exactly the same region of interest), and also monostatic SAF with synthetic transmit focusing.

This is the author's version (accepted manuscript) of a paper that has been published in Ultrasonics, Elsevier.
The final version of record is available at https://doi.org/10.1016/j.ultras.2016.11.022
G. Matrone, A. S. Savoia, G. Caliano, G. Magenes, "Depth-of-Field Enhancement in Filtered-Delay Multiply And Sum Beamformed Images Using Synthetic Aperture Focusing", Ultrasonics, vol. 75, pp. 216-225, March 2017.
DOI: 10.1016/j.ultras.2016.11.022

When employing STA to simulate the scan of a numerical homogeneous phantom in a noise-free scenario, results confirm that the amplitude loss of F-DMAS images can be compensated by the synthetic transmit focusing of received signals at all depths (Fig. 2d), which makes it possible to improve the image DOF.

We should however point out that in this work DAS and F-DMAS images are compared in terms of speckle maximum values, and not of average image intensities, which would be lower for F-DMAS. This is due to the fact that F-DMAS improves the image contrast resolution, which turns out into a better defined speckle pattern, with many more dark areas. Therefore, to compare the intensities of DAS and F-DMAS images, speckle "peaks" should be used, and not "valleys", which usually reach a lower intensity value with F-DMAS.

We also show that, even in the case of a real ultrasound scan, the results confirm our initial assumption (Fig. 3), but not always in a straightforward way. Actually, in fact, when synthetic transmit focusing is applied, the amplitude of experimental F-DMAS images can still decrease at higher depths compared to DAS (Fig. 4d).

This is due to the fact that decorrelations among the backscattered signals – which turn into an intensity drop in F-DMAS images – can be due not only to a misalignment of the received signals during the beamformation process, but also generally to noise. The addition of synthetic white noise to the acquired images allowed us to further enhance this effect. By comparing the original images to the noisier ones, we have in fact shown that possible residual amplitude losses in F-DMAS images with STA and synthetic transmit focusing in the deeper regions should be related to the improved noise-rejection performance of the F-DMAS beamformer, and not to any residual signal de-focusing. Indeed, it is the higher sensitivity to noise of the spatial cross-correlation function that allows F-DMAS to suppress unwanted clutter better than DAS does. Instead, when the SNR improves and electronic noise lowers, the amplitude loss at higher depths is again compensated for (Fig. 4b), demonstrating also the robustness of F-DMAS to other decorrelation sources.

Measurements on the experimental cyst phantom images show that with F-DMAS the CR is always higher than with DAS, but only when synthetic transmit focusing is implemented the contrast values become more similar at all depths (Fig. 5 and Table 2). This demonstrates that the combined use of STA with synthetic transmit focusing and F-DMAS makes it possible to achieve images with a higher contrast throughout the scan depth.

This is the author's version (accepted manuscript) of a paper that has been published in Ultrasonics, Elsevier.
The final version of record is available at https://doi.org/10.1016/j.ultras.2016.11.022
G. Matrone, A. S. Savoia, G. Caliano, G. Magenes, "Depth-of-Field Enhancement in Filtered-Delay Multiply And Sum Beamformed Images Using Synthetic Aperture Focusing", Ultrasonics, vol. 75, pp. 216-225, March 2017.
DOI: 10.1016/j.ultras.2016.11.022

The SNR and CNR values of F-DMAS are anyway lower than those of DAS, due to the more defined speckle texture, which makes speckle variance increase, as previously pointed out. Probably this effect - which was observed also in other works e.g. on Capon/Minimum Variance beamforming [3,26] or Side Lobe Masking [5] - might be compensated for by applying time averaging [27] or spatial compounding [3] techniques, so that a higher CNR/SNR could be obtained, improving anechoic targets detectability. We foresee to further explore this topic in future works.

In vivo images of the carotid artery also confirm the previous results, showing that with STA and synthetic transmit focusing a more uniform higher quality can be achieved with F-DMAS at all depths.

All in all, however, in a real hardware setup, monostatic SAF could be more easily implemented than STA, as in this case only a single-channel architecture is required, which makes it attractive for its potential low cost and power consumption. Unfortunately, the problem with SAF is that not only the SNR is reduced but also the contrast resolution is low. With this technique in fact, a rectangle-shaped, under-sampled (the pitch is doubled) equivalent aperture is achieved, as shown in [19], which turns into a beampattern with a narrow main lobe, but high side and grating lobes.

Since F-DMAS allows to significantly improve the contrast resolution of B-mode images [8], it is worth investigating how F-DMAS beamforming behaves when used in conjunction to SAF. In Fig. 6 we demonstrate that F-DMAS improves the performance of SAF by lowering the side and grating lobes, still preserving a narrow main lobe; thus, images show a higher definition and contrast (Fig. 7). Actually, however, the strong presence of noise at higher depths compromises the image quality, and F-DMAS images look darker due to the decreased signal coherence. Nevertheless, if we look at single-frame images, where both electronic and acoustical noise affect the image, F-DMAS has a positive impact on system performance and it improves the CR even of the deeper cyst. *In vivo* images with SAF were instead not shown, as in this case the image quality was poor due to the very low SNR. Anyway we shall consider that, in an ad-hoc developed single-channel system, with a transmit/receive-path electronics optimized for such application, probably better performance could be achieved.

On the other hand, F-DMAS would imply higher computational times compared to standard DAS, as it involves more complex operations like the square root and multiplications [8, 28]. Nevertheless, such

This is the author's version (accepted manuscript) of a paper that has been published in Ultrasonics, Elsevier.
The final version of record is available at https://doi.org/10.1016/j.ultras.2016.11.022
G. Matrone, A. S. Savoia, G. Caliano, G. Magenes, "Depth-of-Field Enhancement in Filtered-Delay Multiply And Sum Beamformed Images Using Synthetic Aperture Focusing", Ultrasonics, vol. 75, pp. 216-225, March 2017.
DOI: 10.1016/j.ultras.2016.11.022

operations can be efficiently simplified using approximate solutions and architecture-optimized instructions, as pointed out in [12]. A real-time implementation of F-DMAS is foreseen in future work, and thus also an actual accurate estimation of the required computational effort.

Overall, we have shown that F-DMAS beamforming can potentially make SAF an appealing technique, since adequate contrast and resolution performances could be achieved with a very simple hardware architecture. This represents a first step towards a more in-depth study on the use of F-DMAS in conjunction to alternative SAF schemes, in which few elements may be used by following "smart" activation patterns, which could make it possible to keep the hardware architecture complexity low, optimizing the beam shape at the same time.

ACKNOWLEDGMENT

This work is partially funded by the National governments and European Union through the ENIAC JU under grant agreement number 324257 (DeNeCor Project).

REFERENCES

[1] J.B. Van Veen, K.M. Buckley, Beamforming techniques for spatial filtering, in Wireless, Networking, Radar, Sensor Array Processing, and Nonlinear Signal Processing, CRC Press LLC, 1999.

[2] J.F. Synnevåg, A. Austeng, S. Holm, Adaptive Beamforming Applied to Medical Ultrasound Imaging, IEEE Trans. Ultrason., Ferroelectr., Freq. Control, vol. 54, no. 8, pp. 1606-1613, 2007.

[3] F. Vignon, M.R. Burcher, Capon beamforming in medical ultrasound imaging with focused beams, IEEE Trans. Ultrason., Ferroelectr. Freq. Control, vol. 55, no. 3, pp. 619–628, 2008.

[4] C.H. Seo, J.T. Yen, Sidelobe suppression in ultrasound imaging using dual apodization with cross-correlation, IEEE Trans. Ultrason., Ferroelectr., Freq. Control, vol. 55, no. 10, pp. 2198-2210, 2008.

[5] A.S. Savoia, G. Caliano, G. Matrone, G. Magenes, A. Ramalli, E. Boni, P. Tortoli, Improved lateral resolution and contrast in ultrasound imaging using a sidelobe masking technique, in Proc. IEEE International Ultrasonics Symposium, Chicago, IL, USA, September 2014, pp. 1682-1685.

[6] T. Lo, H. Leung, J. Litva, Nonlinear beamforming, Electronics Letters, vol. 27, no. 4, pp. 350-352, 1991.

[7] A. Trucco, V. Murino, On nonlinear effects of envelope detection in beamforming systems, IEEE Trans. Ultrason., Ferroelectr., Freq. Control, vol. 44, no. 4, pp. 948-952, 1997.

[8] G. Matrone, A.S. Savoia, G. Caliano, G. Magenes, The Delay Multiply and Sum beamforming algorithm in ultrasound B-mode medical imaging, IEEE Trans. Med. Imag., vol. 34, no. 4, pp. 940-949, 2015.

[9] H.B. Lim, N.T. Nhung, E.P. Li, N.D. Thang, Confocal Microwave Imaging for Breast Cancer Detection: Delay-Multiply-and-Sum Image Reconstruction Algorithm, IEEE Trans. Biomed. Eng., vol. 55, no. 6, pp. 1697-1704, 2008.

[10] G. Matrone, A. S. Savoia, G. Caliano, G. Magenes, "Ultrasound plane-wave imaging with delay multiply and sum beamforming and coherent compounding," in Proc. IEEE Conf. Eng. Med. Biol. Soc. (EMBC), Orlando, FL, USA, 2016, pp. 3223–3226.

[11] G. Matrone, A. S. Savoia, G. Magenes, "Filtered Delay Multiply and Sum Beamforming in Plane-Wave Ultrasound Imaging: Tests on Simulated and Experimental Data," in Proc. IEEE International Ultrasonics Symposium, Tours, France, 2016.

[12] G. Matrone, A. Ramalli, A. S. Savoia, P. Tortoli, G. Magenes, "High Frame-Rate, High Resolution Ultrasound Imaging with Multi-Line Transmission and Filtered-Delay Multiply And Sum Beamforming," in IEEE Trans. Med. Imag., doi:10.1109/TMI.2016.2615069.

[13] T.L. Szabo, Diagnostic ultrasound imaging: inside out. Hartford: Elsevier Academic Press, 2004.

[14] G. Matrone, A.S. Savoia, G. Caliano, G. Magenes, Ultrasound Synthetic Aperture Focusing with the Delay Multiply and Sum Beamforming Algorithm, in Proc. 37th IEEE Annual International Conference of the Engineering in Medicine and Biology Society (EMBC), Milan, Italy, August 2015, pp. 137-140.

[15] R. Mallart, M. Fink, The van Cittert-Zernike theorem in pulse echo measurements, J. Acoust. Soc. Am., vol. 90, pp. 2718–2727, 1991.

[16] N. Bottenus, B.C. Byram, J.J. Dhal, G.E. Trahey, Synthetic aperture focusing for short-lag spatial coherence imaging, IEEE Trans. Ultrason., Ferroelectr., Freq. Control, vol. 60, no. 9, pp. 1816-1826, 2013.

[17] M.A. Lediju, G.E. Trahey, B.C. Byram, J.J. Dahl, Short-Lag Spatial Coherence of Backscattered Echoes: Imaging Characteristics, IEEE Trans. Ultrason., Ferroelect., Freq. Control, vol. 58, no. 7, pp. 1377-1388, 2011.

[18] J.A. Jensen, S.I. Nikolov, K.L. Gammelmark, M.H. Pedersen, Synthetic aperture ultrasound imaging, Ultrasonics, vol. 44, pp. e5-e15, 2006.

[19] M. Karaman, P.-C. Li, M. O'Donnell, Synthetic aperture imaging for small scale systems, IEEE Trans. Ultrason., Ferroelectr. Freq. Control, vol. 42, no. 3, pp. 429–442, 1995.

This is the author’s version (accepted manuscript) of a paper that has been published in Ultrasonics, Elsevier.
The final version of record is available at https://doi.org/10.1016/j.ultras.2016.11.022
G. Matrone, A. S. Savoia, G. Caliano, G. Magenes, “Depth-of-Field Enhancement in Filtered-Delay Multiply And Sum Beamformed Images Using Synthetic Aperture Focusing”, Ultrasonics, vol. 75, pp. 216-225, March 2017.
DOI: 10.1016/j.ultras.2016.11.022

[20] S.I. Nikolov, J. Kortbek, J.A. Jensen, Practical applications of synthetic aperture imaging, in Proc. IEEE International Ultrasonics Symposium, San Diego, CA, USA, October 2010, pp. 350-358.

[21] D.–L. Liu, R.C. Waag, About the application of the van Cittert-Zernike theorem in ultrasonic imaging, IEEE Trans. Ultrason., Ferroelectr., Freq. Control, vol. 42, no. 4, pp. 590–601, 1995.

[22] R. Mallart, M. Fink, Adaptive focusing in scattering media through sound-speed inhomogeneities: The van Cittert Zernike approach and focusing criterion, J. Acoust. Soc. Am., vol. 96, no. 6, pp. 3721–3732, 1994.

[23] J.A. Jensen, Field: A Program for Simulating Ultrasound Systems, Med. Biol. Eng. Comput., vol. 34, pp. 351-353, 1996.

[24] J.A. Jensen,N.B. Svendsen, Calculation of pressure fields from arbitrarily shaped, apodized, and excited ultrasound transducers, IEEE Trans. Ultrason., Ferroelectr., Freq. Control, vol. 39, no. 2, pp. 262-267, 1992.

[25] P. Tortoli, L. Bassi, E. Boni, A. Dallai, F. Guidi, S. Ricci, ULA-OP: an Advanced Open Platform for ULtrasound research, IEEE Trans. Ultrason., Ferroelectr., Freq. Control, vol. 56, no. 10, pp. 2207-2216, 2009.

[26] J.F. Synnevåg, A. Austeng, S. Holm, Benefits of Minimum-Variance Beamforming in Medical Ultrasound Imaging, IEEE Trans. Ultrason., Ferroelectr., Freq. Control, vol. 56, no. 9, pp. 1868-1879, 2009.

[27] J.F. Synnevåg, C.C. Nilsen, S. Holm, Speckle Statistics in Adaptive Beamforming, in Proc. IEEE Int. Ultrasonics Symposium, New York, NY, USA, 2007, pp. 1545-1548.

[28] J. Park, S. Jeon, J. Meng, L. Song, J. S. Lee, C. Kim, Delay-multiply-and-sum-based synthetic aperture focusing in photoacoustic microscopy, J. Biomed. Opt., vol. 21, no. 3, pp. 036010.